INTL JOURNAL OF ELECTRONICS AND TELECOMMUNICATIONS, 2026, VOL. 72, NO. 2, PP. 1-6
Manuscript received October 15, 2025; revised April, 2026. doi: 10.24425/ijet.2026.157922

RIS-aided cooperative UAV swarm for mmWave communications in urban environments

Abdulrahaman Alhafid, and Sedki Younis

Abstract—This paper investigates the integration of reconfigurable intelligent surfaces (RIS) mounted on cooperative unmanned aerial vehicle (UAV) swarms to enhance mmWave communication in dense urban environments. While mmWave bands offer large bandwidths for high data rates, their severe path loss and blockage remain major obstacles in practical deployments. UAVs provide flexible line-of-sight (LoS) connectivity, whereas RIS enables programmable reflection to strengthen non-line-of-sight (NLoS) links. By combining these technologies, we develop a proposed framework that determines UAV positions and RIS phase configurations under realistic constraints, including quantized RIS phases, UAV, and flight restrictions. Simulation results demonstrate that RIS-aided UAV swarms significantly improve system reliability compared to single-UAV or non-RIS baselines. The findings reveal that both UAV swarm size and number of RIS elements strongly influence performance: average signal-to-noise ratio (SNR) increases with more UAVs, bit error rate (BER) decreases with RIS enlargement, and outage probability exhibits a steep once the number of UAVs and RIS elements is reached a certain limits. In particular, swarms of four to five UAVs with 16–20 RIS elements achieve outage probabilities below 0.05, ensuring near–ultra-reliable communication while balancing energy and hardware costs. These results confirm that cooperative RIS-enabled UAV swarms are a promising solution for robust mmWave coverage in urban 6G networks.

***Keywords*—Reconfigurable Intelligent Surface (RIS); Unmanned Aerial Vehicles (UAVs); mmWave Communication**

I. INTRODUCTION

UNMANNED Aerial Vehicles (UAVs) are envisioned to play a transformative role in the design and deployment of sixth-generation (6G) non-terrestrial networks (NTNs), driven by their intrinsic versatility, mobility, and capability to operate seamlessly across diverse environments [1]. Owing to their high maneuverability and cost-efficient deployment, UAVs are increasingly recognized as promising aerial communication platforms, capable of significantly enhancing the coverage, capacity, and energy efficiency of contemporary wireless networks [2][3]. Conversely, the integration of UAVs into cellular networks as aerial users is anticipated to substantially improve network reliability and throughput. This is primarily attributed to their high probability of establishing line-of-sight (LoS) wireless connections, which leads to superior air-to-ground communication quality [4]

To overcome unfavorable propagation conditions and enhance overall communication performance, reconfigurable intelligent surfaces (RISs) have recently garnered considerable research interest [5]. A RIS typically consists of a large number of low-cost and energy-efficient reconfigurable reflecting elements, each capable of manipulating the incident electromagnetic wave by applying a controllable phase shift. By intelligently coordinating the phase shifts of all elements, the reflected signals from multiple paths can be coherently combined at the intended receiver, thereby reinforcing the received signal strength, improving link reliability, and ultimately enhancing the achievable data rate [6][7][8][9].

It is important to highlight that, unlike conventional amplify-and-forward relays, a RIS operates by passively reflecting the incident signals through its reconfigurable elements, thereby resulting in significantly lower energy consumption. Moreover, since RISs do not require dedicated transmitter modules and their constituent elements are inherently low-cost [10], the overall implementation cost is considerably reduced. An additional advantage lies in their natural capability to operate in full-duplex mode without the need for complex self-interference cancellation mechanisms, further simplifying system design [11][12].

The integration of RIS technology with UAV platforms leverages the complementary advantages of both technologies to establish highly reconfigurable communication environments. This synergy is anticipated to significantly improve coverage, reliability, spectral efficiency, and energy efficiency in next-generation wireless networks. So, in recent years, increasing research efforts have been directed toward the integration of RIS with UAV-based communication systems, which has consequently garnered considerable attention. For instance, several studies have reported performance analyses of RIS-assisted UAV communication systems [13]. In [14], the outage probability of RIS-assisted UAV communications is analyzed under two paradigms: (i) UAV-aided communication, where a UAV operates as an aerial BS with RIS support for A2G links, and (ii) cellular-connected UAV communication, where the UAV functions as an aerial UE served by a ground BS with RIS support for G2A links. In both cases, the UAV–RIS channels are modeled using Rician fading. Another scheme involving the installation of a RIS on a UAV was first introduced in [15], where the authors focused on employing reinforcement learning to optimize the downlink

Abdulrahaman Alhafid is with the Department of Communications and Intelligent Digital Systems Engineering, College of Engineering, University of Mosul. (e-mail: abdulrhman.alhafid@uomosul.edu.iq).

Sedki Younis is with the Department of Computer and Information Engineering, College of Electronics Engineering, Ninevah University, Mosul. (e-mail: sedki.thanoon@uoninevah.edu.iq).

communication capacity. In [16], the authors presented a performance analysis of a UAV communication system equipped with a RIS, with particular emphasis on evaluating the impact of UAV altitude and location. In [17], the authors of the paper investigated the integration of UAV communication with beyond diagonal RIS in 6G NTNs. They addressed the potential of integration, presented a case study on transmissive beyond diagonal RIS communication mounted on a UAV, and identified key research directions for future work. The authors in [18] investigated the deployment of multiple UAVs each with RIS panel for improving hotspot coverage of mmWave communication and proposed a Thompson sampling-based algorithm for maximizing the data-rate and minimizing the UAV flight energy consumption under budget and collision constraints. In [19], the authors of the paper investigated a UAV-mounted on intelligent reflecting surface (IRS) for improving mmWave communication in low-altitude urban environments. They jointly optimized the rate and minimized the energy consumption of the UAV-mounted IRS using a deep reinforcement learning algorithm for solving a non-convex problem.

In this work, we present a comprehensive performance analysis of a communication system assisted by RISs mounted on UAVs. Considering complex urban environments, buildings and other obstacles can block LoS communication links between base station (BS) and ground users, which severely degrades channel quality. To overcome this limitation and improve BS-user connectivity, this paper considers the use of a swarm of UAVs, each equipped with a RIS. A similar system configuration using only one UAV was examined in [15] and [16], where in the former the authors studied a UAV-assisted RIS uplink system from an optimization perspective rather than a detailed performance analysis. They focused on secure energy efficiency maximization by jointly optimizing the UAV trajectory, RIS phase configurations, user association, and transmit power allocation. While in the latter, the authors analyzed a UAV-assisted RIS communication system under blocked direct links and Rician fading channels. They proposed two approximate statistical models for the cascaded channel, optimized the UAV's altitude and placement, and assessed performance through outage probability, bit error rate (BER), and average sum-rate. Distinguishing from these studies, our work considers the optimization of RIS phase configurations for each UAV in the swarm along with UAV trajectories for downlink system, under distinct fading conditions for the BS–UAV and UAV–user channels, while assuming that the direct link is blocked.

The main contributions of the paper can be summarized as follows. First, we propose an optimal phase shift design for the RIS deployed on the UAV swarm. We ensure that the signal reflected by the RIS reaches the user with constructive phase shift while taking into account various practical constraints. Second, we propose an energy-aware UAV positioning and trajectory design that minimizes the distance traveled by the UAV swarm to its optimal positions. We reduce the energy consumption of the UAVs without degrading the channel conditions. Finally, we provide a thorough performance analysis of the RIS-based UAV swarm system with varying RIS sizes and different UAV swarm configurations. The performance of the system is assessed in terms of outage probability and BER. It is shown that the RIS-based system can be used to improve the performance of the system.

The rest of the paper is organized as follows. Section II introduces the system model and problem formulation. Section III provides the proposed algorithm. Section IV provides the performance analysis. Section V provides the simulation results. Section VI provides the conclusion.

II. SYSTEM MODEL AND PROBLEM FORMULATION

A. *System Model:*

Consider a transmitting BS that serves user equipment (UEs) over the downlink using mmWave frequencies. Under LoS conditions, downlink communication is generally reliable and efficient. However, in the presence of blockages (which is the case considered in this paper) the propagation attenuation increases significantly, thereby degrading link quality. To mitigate this issue and enhance the received signal power, we propose deploying a swarm of UAVs, each equipped with a RIS, to assist in serving non-line-of-sight (NLoS) UEs.

As illustrated in Fig. 1, the presence of tall buildings creates a NLoS channel between the BS and the users. To address this, K of UAVs each equipped with a RIS is employed as a passive reconfigurable reflector to assist the communication between the BS and the UEs. The RIS is composed of $N \times N$ reflecting elements, each capable of applying a controllable phase shift. By reflecting the mmWave signals from the BS toward the UEs, the RIS effectively transforms the obstructed NLoS link into two cascaded LoS links. Furthermore, mounting the RIS on a UAV enables dynamic adjustment of its position and the trajectory for each one is optimized to ensure LoS and strong end-to-end signal-to-noise ratio (SNR) connectivity between the BS and the UEs.

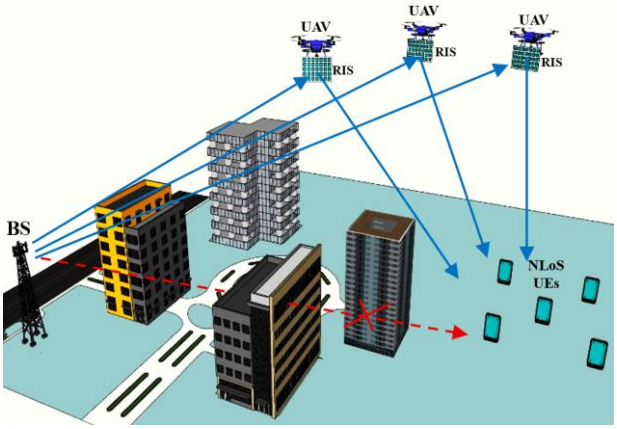

Fig. 1. System Model

Each UAV usually flies at relatively fixed high altitude h. The UAV trajectory is discretized into time slots. It is assumed that the maximum flight duration is T, which is the time to reach the optimal final position. For analytical tractability, the flight duration is discretized into M equally spaced time slots of length δ, such that $T = M\delta$. Let $\mathcal{M} = \{1,2,\dots,M\}$ denote the set of discrete time slots, the horizontal position of the k^{th} UAV at time slot $t \in \mathcal{M}$ is given by $\boldsymbol{p_k}[t] = [x_k(t), y_k(t)]^T$. To ensure feasible mobility, the UAV trajectory dynamics follow a basic kinematic model to satisfy the velocity constraint.

$$\left|\left|\boldsymbol{p}_k(t+1)-\boldsymbol{p}_k(t)\right|\right| \le \delta.V_k, \forall\, t \in \{1,\dots,M-1\} \quad (1)$$

where V_k denotes the maximum speed of the k^{th} UAV. In addition, the trajectory is subject to initial and final position constraints, $\boldsymbol{p}_k(1)=\boldsymbol{p}_{k-init},\ \boldsymbol{p}_k(M)=\boldsymbol{p}_{\mathrm{k-final}}$

The channel between the BS and the RIS and between the RIS and the UE are assumed to consist of both LoS and scattered multipath components and is therefore modeled using a Rician fading distribution. As shown in [20][21][22], the RIS attains its strongest channel gain when positioned in proximity to either the transmitter or the receiver. Accordingly, the UAV is initially deployed near the target service area to ensure a reliable LoS condition. In this study, we consider the far-field propagation scenario, in this assumption the BS–RIS distance d_{BR} is equal to the distance between the BS and any element of the RIS, i.e., $d_{BR}=d_{BR_n}$. In same manner, the RIS-UE distance can be expressed as $d_{RU}=d_{R_nU}$, where R_n is the n^{th} element of the RIS. Considering blocked LoS communication link between BS and UE, the received signal by the UE can be expressed by the cascaded BS–RIS and RIS–UE channels as:

$$y=\left[\sum_{n=1}^{N} h_{UR_{k,n}} e^{j\psi_n} h_{BR_{k,n}}\right] x + w \quad (2)$$

where $\psi_n \in (0,2\pi)$ represents the phase shift adjustment of the n^{th}element, x is the transmitted symbol with unit average power, $w \sim \mathcal{CN}(0,\sigma^2)$ represents the additive white Gaussian noise (AWGN) with zero mean and σ^2 variance. The channel coefficient between the k^{th}RIS (or UAV) and UE is denoted as:

$$h_{UR_k}=\sqrt{\rho d_{UR_k}^{-\alpha}}\,\mu_n e^{-j\psi_{RU}} \quad (3)$$

where ρ denotes the path loss at the 1m reference distance, $d_{UR_k}=\|\boldsymbol{p}_k-\boldsymbol{p}_{UE}\|$ is the distance between the k^{th} UAV and UE, α is the path-loss exponent, and μ_n denotes the multipath fading coefficients modeled as an independent Rician random variable, ψ_{RU} is the phases of the channel coefficients. Similarly, the channel coefficient between the BS and the k^{th}RIS which are separated by distance $d_{BR_k}=\|\boldsymbol{p}_k-\boldsymbol{p}_{BS}\|$ is denoted as:

$$h_{BR_k}=\sqrt{\rho d_{BR_k}^{-\alpha}}\,\mu_n e^{-j\psi_{BR}} \quad (4)$$

As a result, the received SNR at the UE can be expressed as:

$$\mathrm{SNR}=\frac{P_t\left|\sum_{n=1}^{N} h_{R_{k,n}U}\, e^{j\psi_n} h_{BR_{k,n}}\right|^2}{\sigma^2} \quad (5)$$

where P_t is the transmitted power. Consequently, as in [13], the maximum instantaneous SNR at the UE can be expressed as:

$$\mathrm{SNR}=\frac{P_t\left|\sum_{n=1}^{N} h_{R_{k,n}U} h_{BR_{k,n}}\right|^2}{\sigma^2} \quad (6)$$

B. Problem Formulation

The objective of this work is to maximize system performance by optimizing the UAVs' two-dimensional trajectories toward their final positions and the phase shifts of the RISs. Specifically, system performance is characterized by the end-to-end SNR of the BS-to-UE communication path, which is enhanced through cooperative RIS-enabled UAVs. Accordingly, the optimization problem can be formulated as:

$$\max_{\boldsymbol{\theta}_k,\boldsymbol{p}_k}\ SNR = f(\boldsymbol{h}_{BR},\boldsymbol{h}_{RU},\boldsymbol{\Theta}_k) \quad (7)$$

where vectors $\boldsymbol{h}_{BR}\in\mathbb{C}^{N\times 1}$ and $\boldsymbol{h}_{RU}\in\mathbb{C}^{N\times 1}$ denote the BS–RIS and RIS–UE channel coefficients, respectively, $\boldsymbol{\Theta}_k$is the diagonal matrix contains the phase shifts applied by the reflecting elements of the k^{th} RIS.

$$\boldsymbol{\Theta}_k=\mathrm{diag}\left(e^{j\psi_{k,1}},\ e^{j\psi_{k,2}},\dots,\ e^{j\psi_{k,N}}\right) \quad (8)$$

Therefore, the optimization variables are defined as the UAV trajectories (including the final UAV positions) and the RIS phase-shift matrices, expressed as:

$$\{\boldsymbol{\psi}_k^{\star}\}_{k=1}^{K},\ \{\boldsymbol{p}_k^{\star}\}_{k=1}^{K} \quad (9)$$

III. PROPOSED ALGORITHM

We adopt an alternating optimization strategy: UAV placement is optimized using successive convex approximation (SCA), and RIS phase optimization is performed iteratively to maximize constructive reflection. The proposed SCA iteratively solves the non-convex joint problem and converges to a locally optimal stationary solution, with computational complexity scaling with the number of UAVs and RIS elements. The optimization is subject to practical constraints including: (i) UAV energy budgets: flight energy consumption and maximum displacement limits, communication-related energy (maintaining RIS operation, control signaling). (ii) UAV flight envelope limits: $x_k\in[x_{min},x_{max}]$, $y_k\in[y_{min},y_{max}]$. ii) No-fly zone (NFZ) or blockage regions constraint: In urban environments, UAV trajectories are constrained by regulatory no-fly zones, physical blockages such as tall buildings, and safety restrictions, requiring UAV positions to avoid restricted regions while maintaining feasible relay paths. iv) UAV mobility constraint which is explained in equation (1). v) RIS hardware limitations: to reduce RIS complexity (phase shifters, varactors, PIN diodes), elements made to realize arbitrary continuous phase shifts, i.e., each RIS element is restricted to discrete phase levels, depending on the number of quantization bits b, so:

$$\psi_{k,n}\in Q_b=\left[0,\frac{2\pi}{2^b}\ \dots,\frac{2\pi(2^b-1)}{2^b}\right] \quad (10)$$

The algorithm for the efficient deployment of the UAVs positions and the RIS phase profile for each RIS is summarized in Algorithm 1

***Algorithm 1**: UAV–RIS Alternating **Optimization** Algorithm*

Input: Input: BS position $\boldsymbol{p}_{BS}$, users $\{\boldsymbol{p}_{UE}\}$, buildings NFZ set $\mathcal{F}_{\text{NFZ}}$, RIS bits b, RIS elements N_k, bounds $[x_{min}, x_{max}]$, $[y_{min}, y_{max}]$, UAV direction grids and step size, tolerance ε, max iters I_{max}

Output: UAV trajectory and optimum positions $\{\boldsymbol{p}_k^\star\}$, RIS phases $\{\boldsymbol{\psi}_k^\star\} = [\psi_{k,1}, \psi_{k,2} \dots \psi_{k,N}]$.

1: **Initialize:** Initialize UAV positions $\boldsymbol{p}_{k-init}$ and RIS phases $\boldsymbol{\psi}_{k-init}$.

2: Set t ← 0

3: Repeat:

- Solve for $\boldsymbol{p}_k(t+1)$ with fixed $\boldsymbol{\psi}_k(t+1)$. Subject to: UAV flight envelope constraints, NFZ avoidance.
- Update RIS phase for each UAV
- Computing the utility $f(t+1)$
- t ← t + 1

3: *Until* $\frac{|f(t)-f(t-1)|}{|f(t-1)|} < \varepsilon$ *or* $t \geq T$

Return: $\{\boldsymbol{p}_k^\star\}$,$\{\boldsymbol{\psi}_k^\star\}$

IV. PERFORMANCE METRICS

To assess the reliability and quality of a digital communication system under noise and fading conditions, suitable performance metrics must be employed. In this work, the key metrics considered are outage probability and average BER. The outage probability is a widely used metric for evaluating the reliability of wireless communication systems. It is defined as the probability that the instantaneous received SNR being smaller than a specified threshold SNR_{th}, which corresponds to the cumulative distribution function (CDF) of the SNR evaluated at SNR_{th} [23]. According to (6), the instantaneous SNR can be expressed as,

$$SNR = \frac{P_t \left|\sum_{i=1}^{N} h_{R_n U} h_{BR_n}\right|^2}{\sigma^2} = \overline{SNR}\chi^2 \tag{11}$$

where $\overline{SNR} = \frac{P_t}{\sigma^2}$ is the average SNR, and $\chi = \left|\sum_{i=1}^{N} h_{R_n U} h_{BR_n}\right|$

$$P_{outage} = P_r(SNR \leq SNR_{th}) = P_r\left(\sum_{i=1}^{N} h_{R_n U} h_{BR_n} \leq \frac{SNR_{th}}{\overline{SNR}}\right) \tag{12}$$

Another important parameter in communication systems, and often the most difficult to evaluate, is the average BER. It reflects the performance in terms of the reliability of information transmitted on average in the presence of variations in the channel conditions. Assuming that the instantaneous SNR is represented by γ, the unified formula for the average BER in different binary modulation schemes is given in [24].

$$BER_{Avg} = \frac{q^p}{2\Gamma(q)} \int_0^\infty \exp(-q\gamma)\, \gamma^{p-1} F(\gamma) d\gamma \tag{13}$$

Here, $\Gamma(\cdot)$ denotes the Gamma function, while the parameters p and q specify the modulation scheme. For instance, in the case of binary phase-shift keying (BPSK), which is adopted in this work, $p = 0.5$ and $q = 1$.

V. NUMERICAL AND SIMULATION RESULTS

In this section, the effectiveness of the proposed algorithm is validated through numerical simulations. As illustrated in Fig. 2, we consider a square area of $500\,m \times 500m$ with the BS located at the origin, $\boldsymbol{p}_{BS} = (0,0)$. The users are uniformly distributed within the first quadrant of the area, bounded by the coordinates (250,250), (500,250), (500,500) and (250,500). A total of $K = 6$ UAVs, indexed by $k = \{1,2,\dots,6\}$, are initially deployed in a straight line at a fixed altitude, with equal spacing. Their initial positions are represented by blue diamonds, where the first and last UAVs are located at $\boldsymbol{p}_{1-init} = (50,250)$ and $\boldsymbol{p}_{6-init} = (450,250)$, respectively. The optimized final UAV positions are indicated by green diamonds. The UAV trajectory step size is set to $5\,m$.

Each UAV is equipped with a RIS consisting of $N_k \in \{8{:}\,28\}$ reflecting elements. To reduce complexity, the RIS elements are quantized with a resolution of $b = 2$ bits. Unless otherwise specified, the simulation parameters are as follows: carrier frequency of $28\,GHz$, BS transmit power of 1 watt, noise power density $N_0 = -90\,dB$, path-loss exponent $\mu_n = 2.2$, Rician K-factor of 5, and an outage threshold of $10\,dB$. All results are obtained using 1000 independent Monte Carlo realizations and are averaged over independent channel realizations

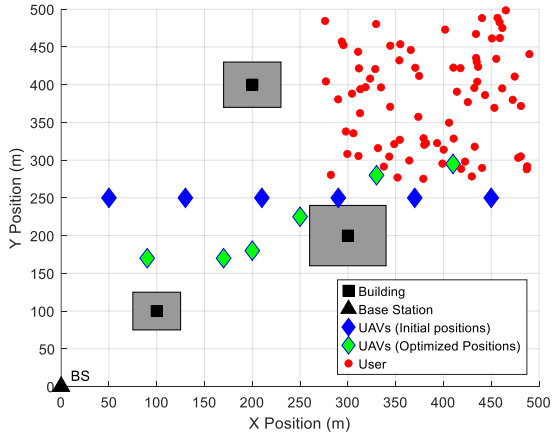

Fig. 2. Illustration of the proposed system model.

The average SNR variation with the number of UAVs for different RIS sizes is obtained in Fig. 3. As expected, the increasing of UAVs number in the swarm can improves the average SNR. That because additional UAVs will provide more reflection opportunities, which provide better coverage and mitigate blockage effects. The advantage is more pronounced for larger RIS panels due to the increased array gain. However It is also observed that the improvement diminishes and exhibits flooring when the swarm size increased to a certain number indicating the marginal contribution becomes less pronounced.

This highlight the trade-off between the number of UAVs in the swarm and the RIS panel size, i.e., the same performance may also be achieved using fewer UAVs but with a larger RIS panel size. This is an important consideration in terms of energy and cost efficiency in RIS-aided UAV urban environments. This reveal a trade-off between the swarm size and the RIS panel size. In other words, comparable performance can be obtained by equipping less UAVs but with larger RIS panels. This is an important observation to achieve an efficiency in term of energy and cost for RIS-aided UAV in urban environments.

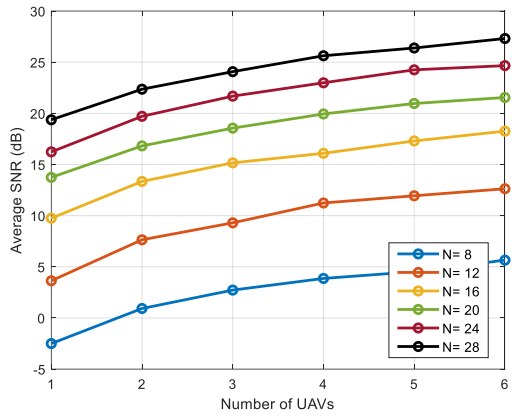

Fig. 3. Average SNR versus the number of UAVs for different RIS elements.

Fig. 4 presents a plot of BER performance against the RIS size, i.e., the number of RIS elements, per UAV for different UAV swarm sizes. It can be noted that BER performance improves significantly by increasing the size of the RIS. Additionally, increasing the UAV swarm size provides considerable additional gains. For example, at $N = 12$, it can be observed that the BER performance achieved by six UAVs is about four orders of magnitude better than that achieved by a single UAV. Notably, it can be observed that when a single UAV is used, increasing the size of the RIS provides diminishing returns and get flooring after a certain value. This again verifies that spatial diversity offered by UAV swarms and array gain offered by increasing RIS size are critical to providing ultra-reliable mmWave urban communication. Notably, a swarm of five or more UAVs with an RIS of size $N = 16$ can provide near error-free communication.

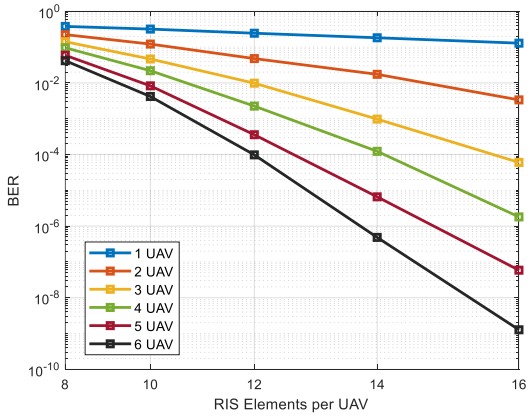

Fig. 4. BER versus the number of RIS elements per UAV for different UAV swarm sizes.

The outage probability as a function of the number of RIS elements per UAV is depicted in Fig. 5 for different swarm sizes. It can be concluded from the figure that the increasing in the number of RIS elements can greatly minimizes outage probability. Moreover, it can be observed that further improvement can be achieved by increasing the swarm size. It can be seen that when a single UAV is employed in the swarm, the outage probability remains higher even when the number of RIS elements is large, which again confirms that the increasing in the number of RIS elements only is not sufficient to reduce outage probability. However, by leveraging the cooperative diversity achieved by the swarm of UAVs, it can be noticed that the outage probability is greatly improved by the increasing in the number of RIS elements per UAV. For example, when the number of UAVs in the swarm is three, it can be observed that the outage probability can be reduced to less than 0.1 when 21 RIS elements per UAV are employed, whereas the outage probability can be reduced to less than 0.05 when 22 or greater RIS elements per UAV are employed. Furthermore, when four UAVs are employed in the swarm, it can be seen that the outage probability can be reduced to less than 0.05 when 20 RIS elements per UAV are employed, whereas the outage probability can be reduced to nearly zero when 22 or greater RIS elements per UAV are employed. Moreover, when five and six UAVs are employed in the swarm, the outage probability can be reduced to less than 0.05 when 18 RIS elements per UAV are employed, whereas the outage probability can be reduced to nearly zero when 18 RIS elements per UAV are employed in the swarm.

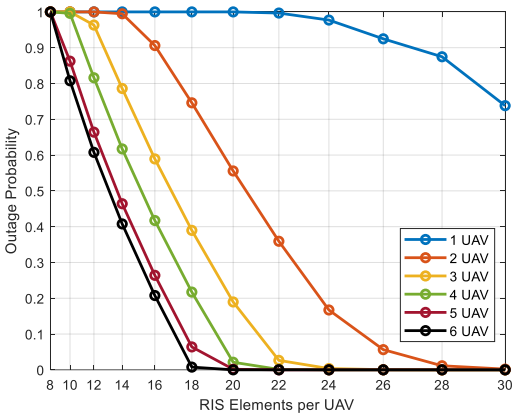

Fig. 5. Outage probability versus the number of RIS elements for different UAV swarm sizes.

VI. CONCLUSION

This paper aimed to investigate the potential of a cooperative UAV swarm, where each UAV is equipped with a RIS, in improving mmWave communications in dense environments. The optimization problems for UAV and RIS are addressed under a number of practical limitations. The simulation results revealed a number of important observations and conclusions, such as the fact that the number and size of the UAV swarm and RIS, respectively, are significant factors in improving the reliability and quality of the mmWave communications. The average SNR increases with the number of UAVs, and the improvement rate diminishes at larger number of UAVs in the swarm. The analysis on the BER revealed that the overall performance is extremely improved by leveraging the benefits

of diversity provided by the UAV swarm and the large number of RIS elements, whereas the performance is limited if a single UAV is used with a large number of RIS elements. The results on the outage probability revealed that there is a reliability effect, where the performance is improved gradually until a specific threshold is reached, and then the outage probability drops sharply to zero if the RIS panel and UAV number are increased further. The UAV swarm consisting of four UAVs and a RIS consisting of 20 elements provide outage probabilities lower than 0.05, and hence this is a suitable tradeoff between performance, energy efficiency, and complexity. The overall results and analysis reveal that the proposed scenario is a highly effective solution in overcoming the issue of mmWave blocking in dense environments and providing ultra-reliable communications. The potential research directions in this area are investigating trajectory optimization in dynamic network environments, RIS-based integrated sensing and communication (ISAC), and AI-based UAV swarm coordination for to support 6G and beyond networks. Moreover, in view of the limited energy capacity of UAVs, the RIS can be used to harness the energy from the un-reflected part of the mmWave signals and convert it into electrical energy using a rectifier for self-sustainability.

REFERENCES

[1] T. Luan Nguyen, G. Kaddoum, T. Nhu Do, and Z. J. Haas, "Ground-to-UAV and RIS-assisted UAV-to-Ground Communication Under Channel Aging: Statistical Characterization and Outage Performance," *IEEE Transactions on Communications*, pp. 1–13, 2025, https://doi.org/10.1109/TCOMM.2025.3543216.

[2] G. Geraci *et al.*, "What Will the Future of UAV Cellular Communications Be? A Flight from 5G to 6G," *IEEE Communications Surveys and Tutorials*, vol. 24, no. 3, pp. 1304–1335, 2022, https://doi.org/10.1109/COMST.2022.3171135.

[3] X. Pang, N. Zhao, J. Tang, D. Niyato, and K. K. Wong, "Joint Trajectory and Beamforming Optimization for Secure UAV Transmission Aided by IRS," in *13th International Conference on Wireless Communications and Signal Processing, WCSP 2021*, IEEE, 2021, pp. 1–6. https://doi.org/10.1109/WCSP52459.2021.9613308.

[4] X. JIANG, M. SHENG, N. ZHAO, C. XING, W. LU, and X. WANG, "Green UAV communications for 6G: A survey," *Chinese Journal of Aeronautics*, vol. 35, no. 9, pp. 19–34, 2022, https://doi.org/10.1016/j.cja.2021.04.025.

[5] H. T. S. ALRikabi, A. H. Sallomi, H. F. KHazaal, and A. Magdy, "Design and experimental evaluation of a reconfigurable intelligent surface for wireless applications," *Results in Engineering*, vol. 26, no. March, pp. 1–14, 2025, https://doi.org/10.1016/j.rineng.2025.104694.

[6] A. K. Alhafid, S. Younis, and Y. E. M. Ali, "Enhanced Far-Field Localization Scheme Using Multi-RIS and Efficient Beam Sweeping," *Progress In Electromagnetics Research C*, vol. 140, no. January, pp. 163–175, 2024, https://doi.org/10.2528/PIERC23112903.

[7] M. Ahmed *et al.*, "Active Reconfigurable Intelligent Surfaces: Expanding the Frontiers of Wireless Communication-A Survey," *IEEE Communications Surveys and Tutorials*, vol. 27, no. 2, pp. 839–869, 2025, https://doi.org/10.1109/COMST.2024.3423460.

[8] A. K. Alhafid, S. Younis, and Y. E. Mohammed Ali, "Efficient near-field localization aided with reconfigurable intelligent surface using geometric dilution of precision," *Journal of Information and Telecommunication*, pp. 1–23, 2023, https://doi.org/10.1080/24751839.2023.2272488.

[9] A. Kh. Alhafid, Y. E. Mohammed Ali, and S. Younis, "Performance Investigation of RIS Aided Localization with TDoA in the Near-Field," *Mathematical Modelling of Engineering Problems*, vol. 10, no. 6, pp. 2127–2134, 2023, https://doi.org/10.18280/mmep.100624.

[10] M. Di Renzo *et al.*, "Reconfigurable Intelligent Surfaces vs. Relaying: Differences, Similarities, and Performance Comparison," *IEEE Open Journal of the Communications Society*, vol. 1, no. May, pp. 798–807, 2020, https://doi.org/10.1109/ojcoms.2020.3002955.

[11] A. I. Alghannam and A. K. Alhafid, "Performance analysis of Unsolicited Grant Service (UGS) service class in WiMAX voip application," *Journal of Engineering Science and Technology*, vol. 15, no. 3, pp. 1481–1491, 2020. https://jestec.taylors.edu.my/V15Issue3.htm

[12] Q. Wu and R. Zhang, "Towards Smart and Reconfigurable Environment: Intelligent Reflecting Surface Aided Wireless Network," *IEEE Communications Magazine*, vol. 58, no. 1, pp. 106–112, Jan. 2020, https://doi.org/10.1109/MCOM.001.1900107.

[13] S. Li, B. Duo, X. Yuan, Y. C. Liang, and M. DI Renzo, "Reconfigurable Intelligent Surface Assisted UAV Communication: Joint Trajectory Design and Passive Beamforming," *IEEE Wireless Communications Letters*, vol. 9, no. 5, pp. 716–720, 2020, https://doi.org/10.1109/LWC.2020.2966705.

[14] M. Abualhayja'A, A. Centeno, L. Mohjazi, Q. H. Abbasi, and M. Ali Imran, "On the Outage Performance of Reconfigurable Intelligent Surface-Assisted UAV Communications," *IEEE Wireless Communications and Networking Conference, WCNC*, vol. 2023-March, no. April 2024, 2023, https://doi.org/10.1109/WCNC55385.2023.10118821.

[15] Q. Zhang, W. Saad, and M. Bennis, "Reflections in the Sky: Millimeter Wave Communication with UAV-Carried Intelligent Reflectors," in *2019 IEEE Global Communications Conference (GLOBECOM)*, 2019, pp. 1–6. https://doi.org/10.1109/GLOBECOM38437.2019.9013626.

[16] L. Yang, P. Li, F. Meng, and S. Yu, "Performance Analysis of RIS-Assisted UAV Communication Systems," *IEEE Trans Veh Technol*, vol. 71, no. 8, pp. 9078–9082, 2022, https://doi.org/10.1109/TVT.2022.3175964.

[17] W. U. Khan, E. Lagunas, A. Mahmood, M. Asif, M. Ahmed, and S. Chatzinotas, "Integration of beyond Diagonal RIS and UAVs in 6G NTNs: Enhancing Aerial Connectivity," *IEEE Wirel Commun*, vol. 32, no. 3, pp. 56–63, 2025, https://doi.org/10.1109/MWC.001.2400359.

[18] E. M. Mohamed, "Deployment of mmWave multi-UAV mounted RISs using budget constraint Thompson sampling with collision avoidance," *ICT Express*, vol. 10, no. 2, pp. 277–284, 2024, https://doi.org/https://doi.org/10.1016/j.icte.2023.07.011.

[19] W. Xie *et al.*, "Joint Optimization of UAV-Carried IRS for Urban Low Altitude mmWave Communications With Deep Reinforcement Learning," *IEEE Trans. Mob. Comput.*, vol. 25, no. 1, pp. 1381–1397, 2026, https://doi.org/10.1109/TMC.2025.3600682.

[20] M. Raeisi, A. Khaleel, M. C. Ilter, M. Gerami, and E. Basar, "A Comprehensive Design Framework for UE-Side and BS-Side RIS Deployments," *IEEE Wirel Commun*, vol. 32, no. 3, pp. 148–155, 2025, https://doi.org/10.1109/MWC.001.2400142.

[21] Y. Zhang, J. Zhang, M. Di Renzo, H. Xiao, and B. Ai, "Reconfigurable Intelligent Surfaces with Outdated Channel State Information: Centralized vs. Distributed Deployments," *IEEE Transactions on Communications*, vol. 70, no. 4, pp. 2742–2756, 2022, https://doi.org/10.1109/TCOMM.2022.3146344.

[22] A. K. Alhafid, Y. E. Mohammed Ali, and S. Younis, "Far-Field Localization for RIS Empowered Wireless Systems Leveraging Beamforming," *Jordan Journal of Electrical Engineering*, vol. 10, no. 3, pp. 484–499, 2024, https://doi.org/10.5455/jjee.204-1701118386.

[23] S. H. Lin, J. Y. Wang, and X. Hua, "Analysis of Outage Probability and Average Bit Error Rate of Parallel-UAV-Based Free-Space Optical Communications," *Entropy*, vol. 27, no. 6, pp. 1–20, 2025, https://doi.org/10.3390/e27060650.

[24] L. Yang, F. Meng, J. Zhang, M. O. Hasna, and M. Di Renzo, "On the Performance of RIS-Assisted Dual-Hop UAV Communication Systems," *IEEE Trans Veh Technol*, vol. 69, no. 9, pp. 10385–10390, 2020, https://doi.org/10.1109/TVT.2020.3004598.